
[Home](#) [Current Issue](#) [Table of Contents](#)

Comparison of Algorithms for the Localization of Focal Sources: Evaluation with simulated data and analysis of experimental data.

Rolando Grave de Peralta Menendez and Sara Gonzalez Andino

Functional Brain Mapping Lab., Dept. of Neurology, Geneva University Hospital, 1211 Geneva 14, Switzerland.

Acknowledgment: Thanks to Mr. Denis Brunet for expertise in designing the analysis software and Drs Micah Murray, Goran Lantz and Christoph Michel for their comments on previous versions of this manuscript. Research supported by the "Programme commun de recherche en genie biomédicale 1999-2002" and the Swiss National Foundation grant 3100-065232.01.

Abstract:

This paper presents a comparative study of the capabilities of five distributed linear solutions to accurately determine the position of single sources. Two recently developed inverse solutions, LAURA and EPIFOCUS are compared to the Minimum Norm, the column Weighted Minimum Norm and the Minimum Laplacian. The comparison is based on three figures of merit: 1) the number of sources with zero localization error, 2) the maximum localization error, and 3) the average localization error as a function of the source eccentricity. The best results in terms of the three figures of merit are obtained for EPIFOCUS and LAURA. We report for the first time a linear inverse solution (EPIFOCUS) capable of localizing all single sources with zero dipole localization error for a relatively low number of sensors (100). The robustness of EPIFOCUS is additionally evaluated in this paper with noisy synthetic data and experimental recordings in epileptic patients. It is concluded that EPIFOCUS is a robust method to localize single sources with the following advantages over single dipole localization: 1) It is computationally more efficient. 2) It is easily applicable to realistic head models (gray matter selected from MRI). 3) Sources are not restricted to be dipolar. The study described in the paper endorses an important theoretical conclusion: While it is possible to design linear solutions with optimal performance in the determination of the position of single sources, such performance is not warranted if multiple sources are simultaneously active. Consequently, lower dipole localization error is neither a sufficient nor a necessary condition for the performance of a linear inverse solution.

INTRODUCTION

The solution of the electromagnetic inverse problem, i.e. the localization of the generators of the measured EEG/MEG data, remains a challenging problem. The

existence of silent sources producing no external fields makes it theoretically impossible to retrieve arbitrary source configurations. In practice, the discrete nature of the measurement adds some constraints to the reconstruction. Nevertheless, under some restrictive conditions, physiologically plausible generators can be estimated.

In this paper, we consider the source localization problem under the constraint that the generator can be represented by either a point source (dipole) or a larger, but still compact, region of the brain. Under this model it is reasonable to compare linear inverse solutions in terms of the dipole localization error (DLE). We describe two recently developed linear inverse solutions and compare them in terms of the DLE with three previously presented linear inverse solutions. For the sake of reproducibility we use in this comparison the same configuration (sensors, solution space and lead field) considered in ISBET NEWSLETTER #6, December 1995; Grave and Gonzalez, 2000; and Grave et al., 2001.

The first solution, LAURA, based on Local AUtoRegressive Averages, makes no assumption about the number or location of the sources. As a linear distributed solution it can be applied to data generated by single or multiple sources. This approach extends the idea used to develop ELECTRA (Grave de Peralta et al., 2000) where constraints are derived from the physical laws governing currents and potentials in biological media. In LAURA, the existence of a unique solution is granted by compensating the lack of information using physically driven local averages, i.e., the unknown scalar (or vector field) is decaying as a parametric function of the distance as predicted by the electrostatic laws.

The second solution that we consider here coined EPIFOCUS, assumes a single concentrated source with unknown location. In contrast with the dipolar model, the source model considered in EPIFOCUS is allowed to have a certain spatial extent, which is more neurophysiologically plausible in cases of focal epilepsy than assuming the electrical activity to be confined to a point. Since EPIFOCUS is a linear method it requires no nonlinear optimization procedure. It is thus, better suited than the single dipole fitting for irregular solution spaces as those resulting from constraining sources to the gray matter detected from anatomical images.

The capabilities of LAURA and EPIFOCUS to localize the position of concentrated sources are compared in what follows with that of the Minimum Norm solution, the Weighted Minimum Norm solution, and one implementation of the Minimum Laplacian solution. First, we present the results for noise free simulated data. The solution producing the best results (EPIFOCUS) is considered for the analysis of noisy synthetic data and experimental data. The results of the simulation are used to promote the discussion on some theoretical topics related to the design and evaluation of linear distributed solutions. In particular, the capabilities of such methods to adequately retrieve arbitrary source distributions are considered on the framework of the model resolution matrix described in Grave and Gonzalez (1998).

MATERIAL AND METHODS

In this section we first describe the setup used in the simulations as well as the procedure used to generate the noisy and noise free data. We next describe the five inverse solutions examined, to end with a brief description of the figures of merit and the experimental data evaluated.

Configurations used in the computer generated data

For reproducibility and compatibility with previous publications we use a lead field model corresponding to the sensor configuration and solution space described in ISBET NEWSLETTER #6, December 1995, Grave and Gonzalez, 2000, Grave et al., 2001. Namely, a unit radius 3-shell spherical head model (Ary et al, 1981), with solution points confined to a maximum radius of 0.8. The sensor configuration comprises 148 electrodes. The solution space consists of 817 points on a regular grid with an inter-grid distance of 0.133 cm, corresponding to 2451 focal sources.

To study the performance of EPIFOCUS versus the number of electrodes we consider the spherical configuration used in our lab with a variable number of electrodes and 1152 solution points confined to the innermost sphere (radius 0.84) of a four-shell spherical model (Stock, 1986). The lead field is computed using the method of Berg and Scherg (1994).

For the noise free simulations the inverse solutions matrices were applied to the potentials maps produced by all the single sources (columns of the lead field matrix). Uncorrelated random noise in the range $\pm 15\%$ of the amplitude of the noiseless data was added to each electrode to generate the noisy synthetic data.

Linear inverse solutions

In the comparison, we include the five linear inverse solutions sketched below. For an extensive discussion and description of linear inverse solutions see Grave and Gonzalez 1998, 1999. Here we will briefly refer to their mathematical introduction and/or their applications to the bioelectromagnetic field.

a) Minimum Norm (MN) solution. It was introduced by Moore (1920) and Penrose (1955a and 1955b). It is the natural solution for problems without a unique solution and no a priori information. It was initially applied to the neuroelectromagnetic inverse problem by Hamalainen and Ilmoniemi (1984).

b) Weighted Minimum Norm (WMN) solution. Described previously in the book of Lawson and Hanson (1974), WMN is probably one of the more frequently applied solutions second to the MN. The physically sound interpretation of the column normalization (all the sources produce equal size measurements) justifies the wide use of this solution considered in the framework of the NIP by Goronitsky and Rao (1997).

c) Minimum Laplacian (ML) solution. Smoothness is a natural mathematical way to solve ill-posed problems, and ML has been extensively used during past the century (see Philips, 1962 and Wahba 1990 and references therein). Many textbooks refer to this technique in the particular context of inverse problems (Tihonov and Arsenin, 1977; Golberg, 1978, Ripley 1981, etc) as well as the combination of the laplacian with weights (Parker, 1994). It has been also considered for the solution of bioelectromagnetic problems (e.g. Huiskamp and van Osterom, 1988; Messinger-Rapport and Rudy, 1988; van Osterom, 1992; Pascual-Marqui et al., 1995; Wagner et al., 1996; Fuchs et al., 1999). One of the most controversial implementations of this method is probably LORETA, enthusiastically described in ISBET NEWSLETTER #6, December 1995, where some main properties of this implementation were claimed without confirmation which finally proved not to hold (Grave and Gonzalez, 2001)

d) Local Autoregressive Average (LAURA) solution. This parametric solution is described in the appendix and relies in incorporating physically derived constraints into the basic equations used to construct local spatial averages as described in Grave and Gonzalez, 1998, Ripley (1981), and Grave and Gonzalez (1999).

e) EPIFOCUS. Linear inverse (quasi) solution designed to localize concentrated sources with high accuracy (see the appendix for mathematical details). Due to its simplicity, it is particularly well-suited to work with data generated by a dominant (non dipolar) concentrated source and realistic (MRI based) head models (Grave et al. 2001, Lanz et al. 2001).

In the comparison we used the inverse matrices associated with the Minimum Norm (MN) solution, the Weighted Minimum Norm (WMN) solution, and the Minimum Laplacian (LORETA) corresponding to the configuration described above (ISBET NEWSLETTER #6, December 1995, Grave and Gonzalez, 2000 and Grave et al 2001). The inverse matrices associated with LAURA and EPIFOCUS were computed using the same lead field matrix (only available in single precision) according to the equations and details given in the appendix.

Figures of merit used in the comparison

There are at least two alternatives to define the localization error depending on the direct use of the estimated inverse solution (bias in dipole localization) or the modulus of the estimated inverse solution (dipole localization error). The second alternative is used in this paper. For details see Grave et al. (1996).

Since we are interested here in the localization of concentrated sources, we computed for each inverse solution the dipole localization error for all the single dipoles included on the source space. The solutions are compared in terms of the number of sources with zero dipole localization error, the maximum localization error, and the average localization error as a function of the source eccentricity.

RESULTS AND DISCUSSION

Computer generated data without noise

Table I below, shows the results obtained for the five linear inverse solutions under investigation. The three columns of LAURA correspond to three different exponents, that is, linear, quadratic and cubic dependence on the distance. For each solution (columns) we represent the percentage of sources with localization error in the range associated to the row. In all cases the localization error is scaled (divided by the grid size) to yield localization errors in grid units.

According to Table I, EPIFOCUS and LAURA perform better than LORETA, WMN and MN since the percentage of sources with zero error are increased to 94.94% (EPIFOCUS) and 32.35% (LAURA) from 20.52% (LORETA), 14.24% (WMN) and 13.42% (MN). Note that LAURA represents a 12% improvement with respect to LORETA, doubling the amount that LORETA improved with respect to WMN. In addition, the maximum error produced by LAURA and EPIFOCUS is lower than the maximum error obtained with LORETA, WMN, or MN.

	EPI FOCUS	LAURA exp=3	LAURA exp=2	LAURA exp=1	LOR	WMN	MN
[0 - 1)	94.94	32.35	29.38	26.44	20.52	14.24	13.42
[1 - 2)	5.06	63.24	66.10	68.87	75.97	47.33	47.49
[2 - 3)	-	4.41	4.53	4.69	3.47	19.71	18.85
[3 - 4)	-			-	0.04	13.99	12.11
[4 - 5)	-			-	-	4.20	6.24
[5 - 6)	-			-	-	0.53	1.88
[6 - 7)	-			-	-	-	-
Max. Error	1	2.45	2.45	2.45	3.16	5.20	5.48

Table I. Percentage of sources located with error in the corresponding range. Columns: Inverse solution. Rows: Range of the localization error in grid units.

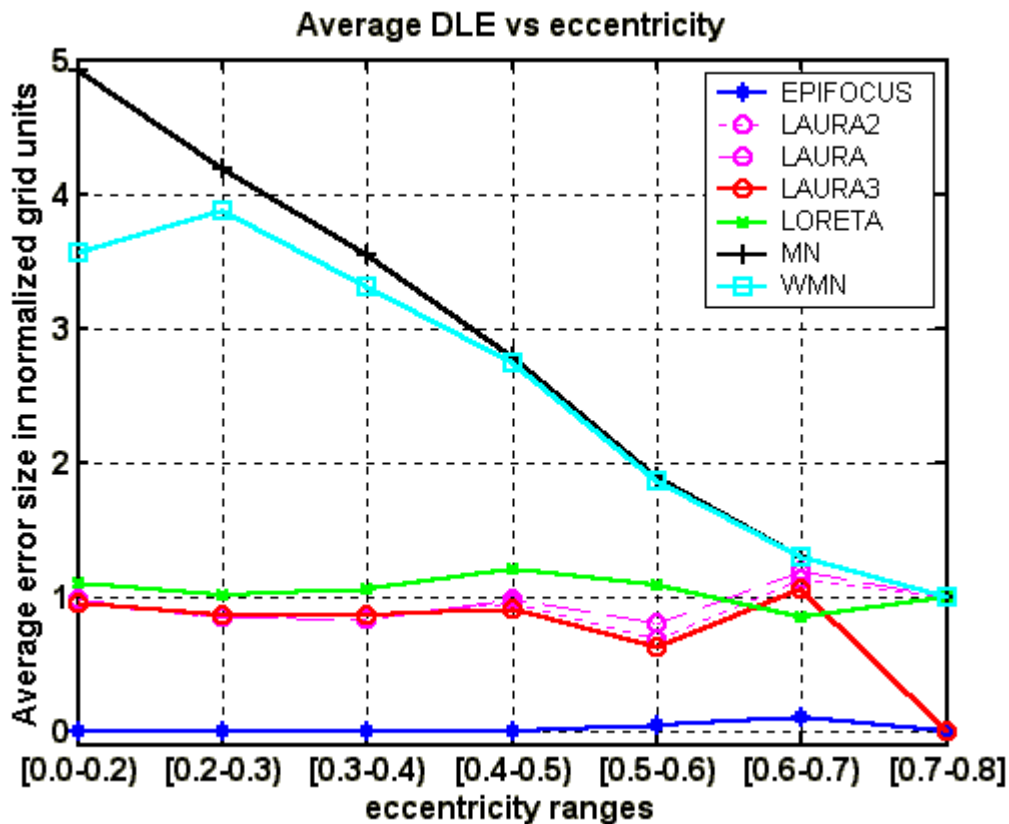


Figure 1. Average localization error as a function of the source eccentricity

In Figure 1 we represent the average localization error as a function of the source eccentricity. As expected the best performance is obtained by EPIFOCUS with nearly zero average error for all eccentricities. LAURA (for all the three exponents) has average error lower than 1 almost everywhere and performs better than LORETA, except for one interval. Both, WMN and MN are the only solutions where a clear dependency on the source eccentricity is observed.

These results clearly show that to minimize the (maximum possible) localization error (independent of the eccentricity) and increase the probability of zero localization error we should use EPIFOCUS or LAURA. However, this conclusion will not necessarily hold for arbitrary source configurations or experimental data. This was illustrated in the comparison presented in Grave (1998) where LORETA and a (radially) Weighted Minimum Norm (Grave and Gonzalez, 1998) were applied to ERP and epileptic data. While both solutions indicated the same number and location of active regions, only some differences on the maxima locations were observed in spite of their different behavior for isolated single sources (ISBET NEWSLETTER #6).

It is important to know how the performance of an inverse solution can change with the source space configuration and the number of electrodes. To evaluate this effect we consider the standard spherical configuration used in our laboratory which comprises 1152 solution points as described in section Material and Methods. Figure 2 presents the results obtained with EPIFOCUS in terms of the number of sources

with zero dipole localization errors for different electrodes configurations containing 25,31,49,68,89,100,131,166 and 181 electrodes respectively.

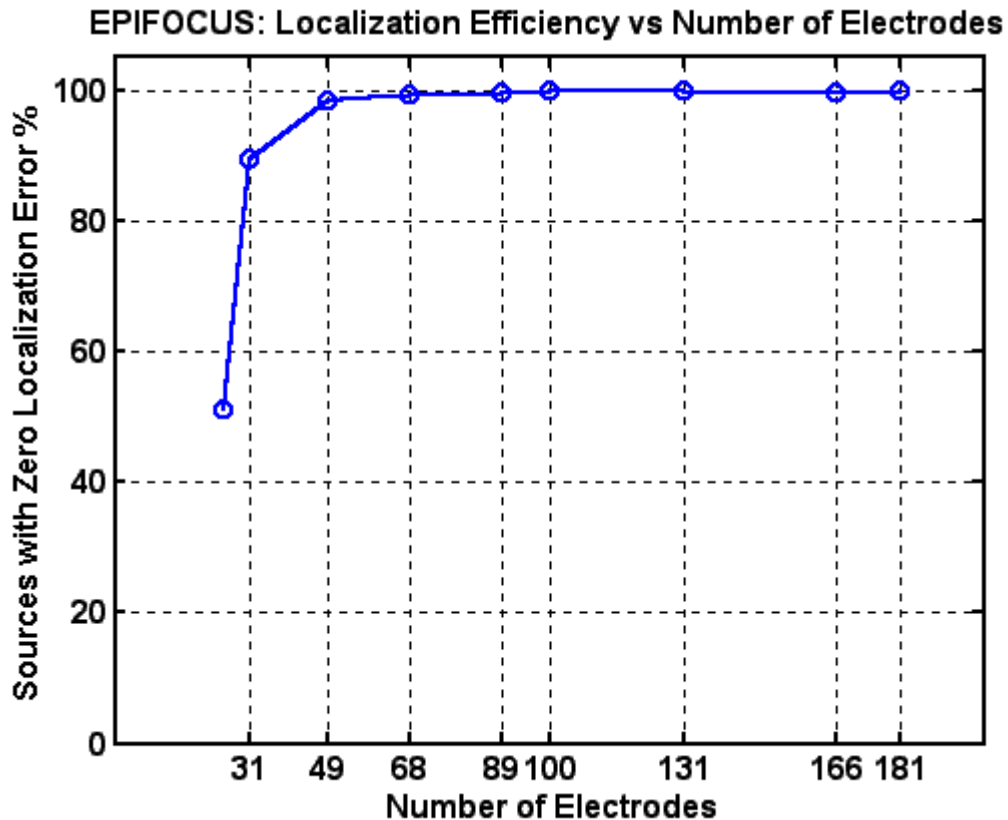


Figure 2. Number of sources with zero localization error vs Number of electrodes for EPIFOCUS

Note that a perfect localization (100%) can be already reached with a relatively low number of electrodes (100). Electrode configurations on this order are becoming a standard in most of the research labs.

Computer generated data with noise

This section cannot include a comparative study for all the solutions considered before due to a lack of data describing the behavior of these solutions in the presence of noise. For that reason, we analyze the noisy data only with EPIFOCUS. As described before the noisy data is obtained by adding to the noiseless data a non correlated noise vector that can change from minus 15% to plus 15% the value at each electrode. Since EPIFOCUS is already a quasi solution, i.e., it does not explain the data, we use the same matrix computed for the noise free data. The results are illustrated in figure 3.

The upper plot of figure 3 shows the empirical probability distribution and the empirical density function for the source localization error. Around the 94% of the sources are still retrieved with zero localization error and the maximum error is no bigger than 2 grid units. The second entry depicts the average localization error that remains very close to zero for all eccentricity values.

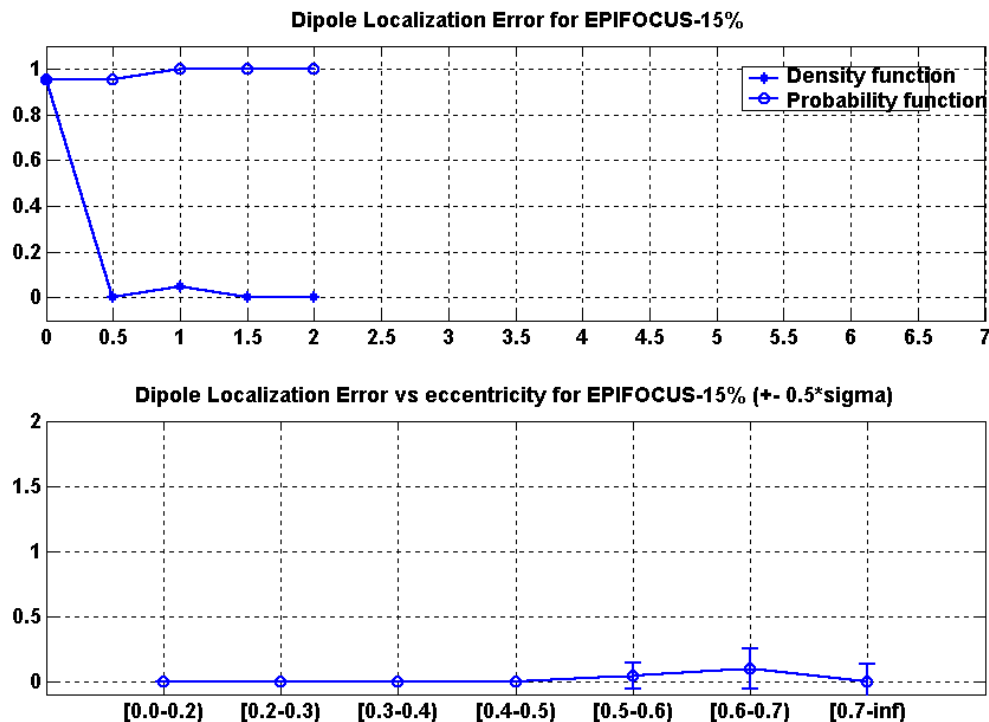


Figure 3. Dipole localization error (DLE) for EPIFOCUS with noisy data. Upper: Probability and density function of the DLE. Lower: Average localization error as a function of the source eccentricity.

Analysis of experimental data

For the analysis of experimental data we consider realistic head models derived from the anatomical MRI of each subject. After segmentation of the anatomical images, a set of solution points belonging to the 3D gray matter distribution is selected. The selected points correspond to an irregular grid of points with distance between 4 to 6 mm. The SMAC method described in Spinelli et al. (2000) is used to locate the electrodes and compute the lead field. With this lead field that summarize all the electrical and anatomical information of the subject we compute the EPIFOCUS inverse as described in the appendix.

In Lantz et al. (2001a), we assessed the sublobar accuracy of EPIFOCUS analyzing the same data where dipolar models (Lantz et al. 1996) and LORETA (Lantz et al. 1997) found no significant differences for the four epileptic sources detected within the temporal lobe. In another study that will be presented elsewhere (Michel et al. in preparation) we analyzed 16 patients with temporal and extratemporal epilepsies. In latter study, we applied EPIFOCUS to increase the accuracy of the localization for those maps where LAURA solution provided a clear evidence of a dominant (concentrated) source. EPIFOCUS results were never in contradiction with the available additional independent information, that is, for the case of visible lesions on the MRI the located source was always within or in the vicinity of the lesion (tumor). For the operated patients, the source was always within the resected area and for all patients where intracranial electrodes were available, the recordings confirmed the source localization results. The following examples discuss the application of EPIFOCUS to two different epilepsy cases: an occipital epilepsy and a temporal lobe epilepsy.

Note that in the following figures, the extent of the activated area is strongly influenced by the simple neighbor interpolation law used to overlay the discrete solution space on the anatomical MRI.

a) Occipital epilepsy

From a methodological (not clinical!) point of view this a really simple case for the inverse solutions. According to the MRI, this patient presented a clear lesion (tumor) on the parieto-occipital region. For the inverse solutions we considered averaged spikes measured on 125 surface electrodes. The results of EPIFOCUS and the Weighted Minimum Norm (WMN) are presented in figure 4. Although both solutions coincide in detecting a clear occipital maximum they slightly differ in the lateralization of it. Probably influenced by the noise, the WMN solution shows a maximum at the left tip of the occipital lobe that extends also to the right. In contrast EPIFOCUS, shows a clear left occipital maxima nearby the MRI lesion, which is not as superficial as the WMN maxima. The fact that the WMN located the focus closer to the brain border than EPIFOCUS coincides with the simulation result of previous section. In spite of this, both inverse solutions are within the resected region and the patient is seizure free.

b) Temporal epilepsy

For this temporal lobe patient an invasive pre-surgical study was carried out since no abnormalities were detected in the structural (MRI) or metabolic images. The EEG study was carried out using 125 surface electrodes, and one sub-dural grid (8x8 contacts) as well as 2 stripes (2x4 contacts and 3x6 contacts) on the right temporal lobe. The intra-cranial data revealed (Lantz et al. 2001b) the temporal propagation of the epileptic discharge from the anterior to the posterior part of the left temporal lobe.

For the inverse solution analysis, a set of averaged spikes measured over the 125 scalp sensors were considered. While in Lantz et al. (2001b) we preprocessed the data (filtering, segmentation and averaging of adjacent maps) before the application of the WMN, here we describe the results of applying the inverse solutions to the raw data resulting from spikes averaging.

Figure 5 shows the localization results obtained for both solutions. The upper left part depicts the superposition of the 125 electrodes waveforms resulting from the averaging process (black traces) and the global field power (GFP) in blue. The three green markers (1,2 and 3) indicate approximately 3 maxima of the GFP corresponding to the latencies where the frontal (1) to posterior (3) transition was detected from the intracranial electrodes. The upper right part depicts the three potential maps at the marker positions and the lower part presents the results of the inverse solutions for the three latencies.

Note that EPIFOCUS clearly identifies the propagation of the seizure discharge (from the anterior to the posterior part of the temporal lobe) coinciding with the intracranial measurements. While from the cortical intracranial grid it is impossible to assess whether the source was at the brain cortex or in a deeper non cortical region, the simulation results induce us to trust the source depth suggested by EPIFOCUS. EPIFOCUS provided consistent localization results for sources everywhere in the brain (deep and cortical) in both noisy and noise free simulations. As we obtained already in Lantz et al. (2001b) the reconstruction provided by the WMN is very superficial and seems to be more sensitive to noisy the data, e.g., the reconstruction for the third latency is too posterior (Figure 5, lower right, third row). After the (standard en bloc) resection of the right temporal lobe the patient is seizure free.

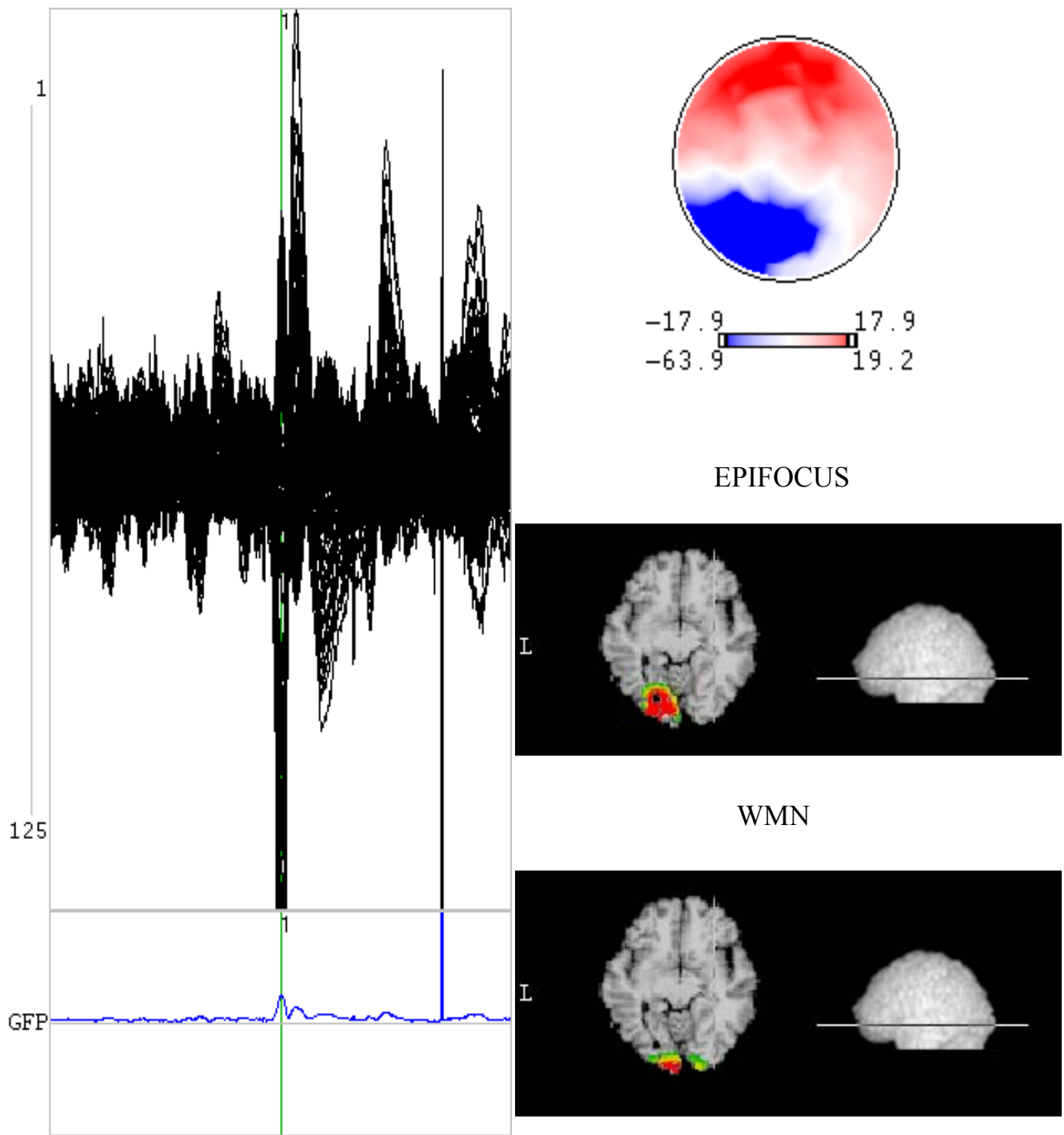
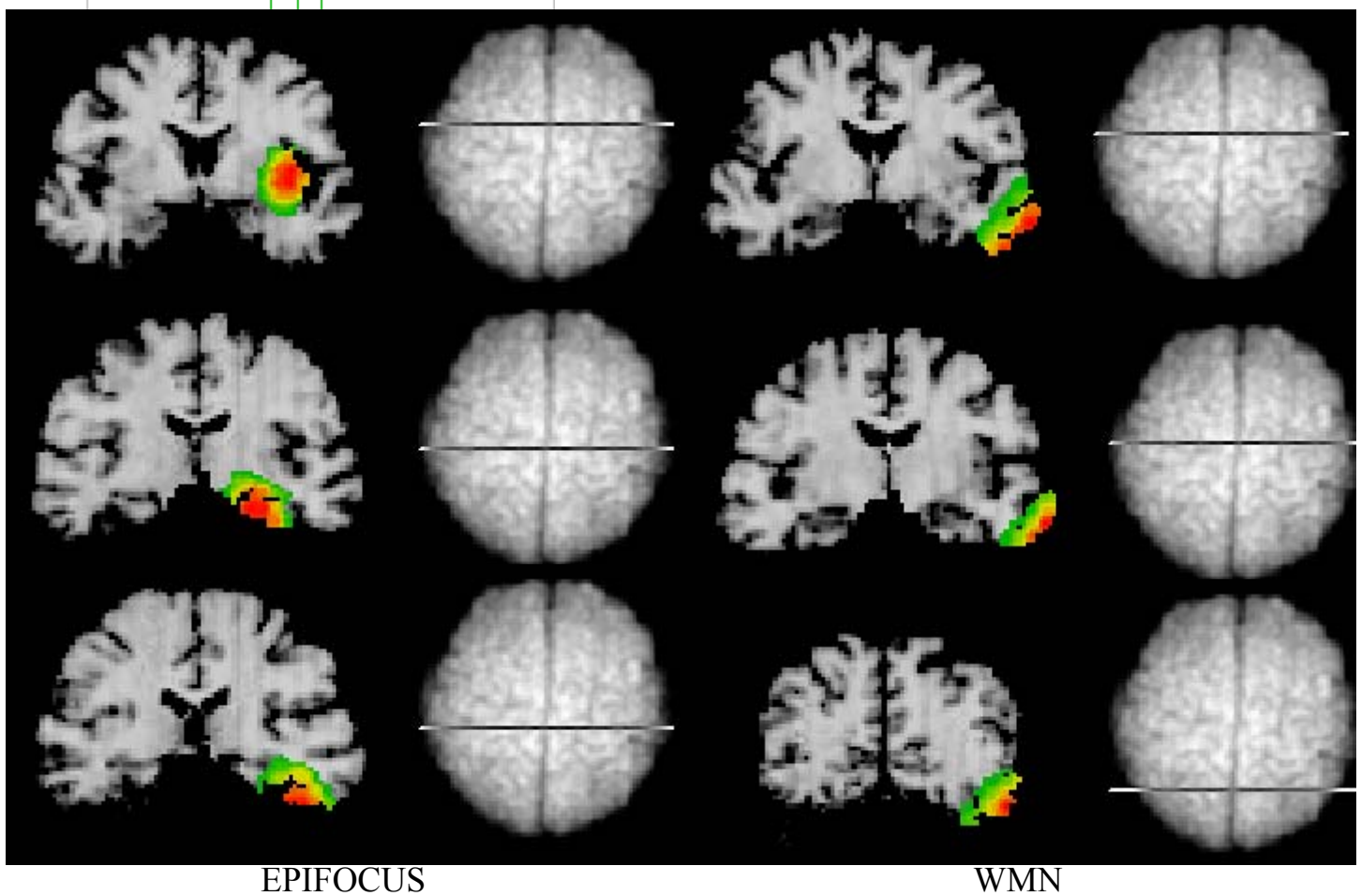
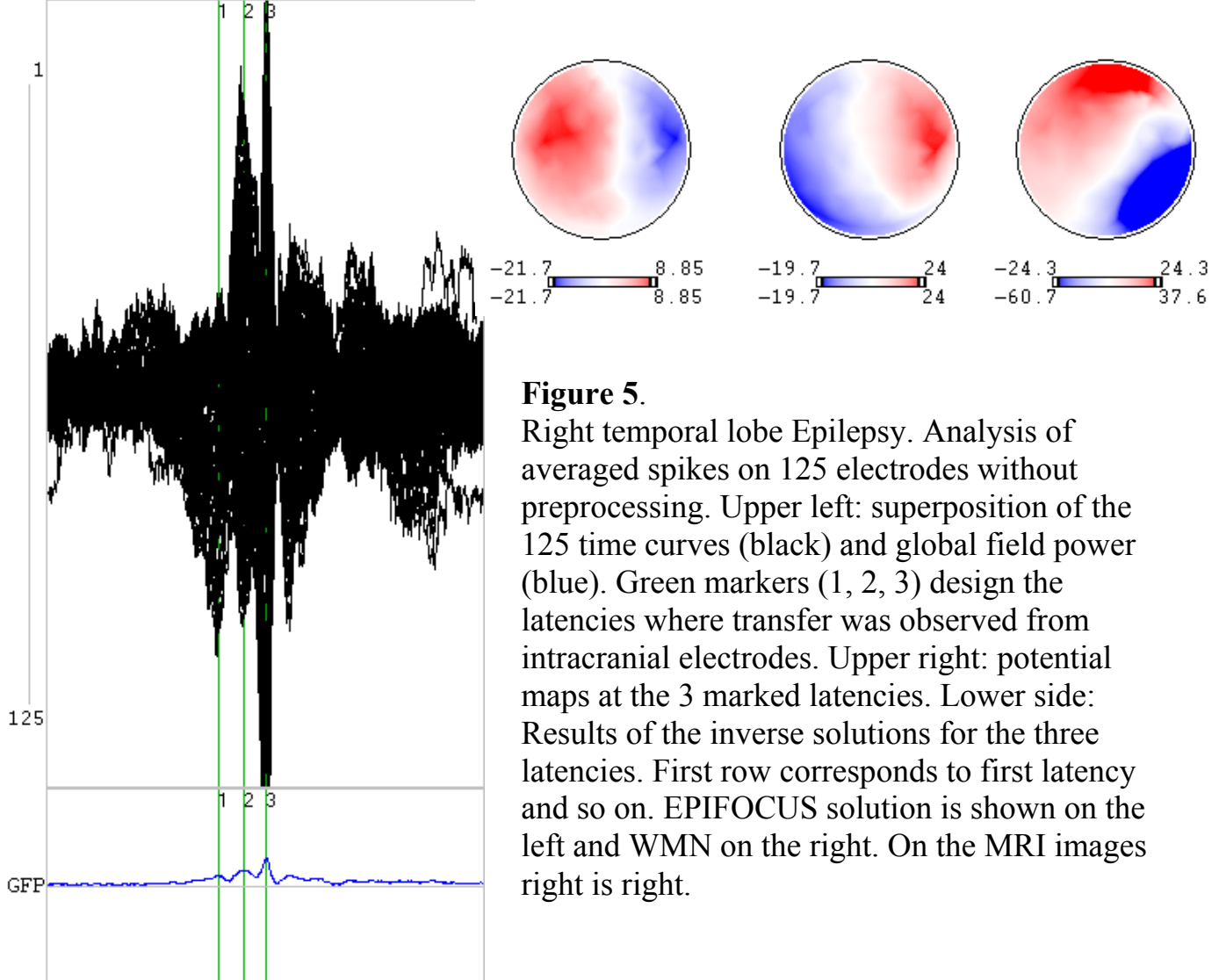


Figure 4.

Occipital Epilepsy. Analysis of averaged spikes on 125 electrodes without preprocessing. The upper left panel shows the superposition of the 125 time curves (black) and lower left the global field power (blue). Green marker (1) designs the latency under analysis. Right side depicts the potential map and the inverse solutions obtained at the marked latency. Only the slice of the maximum is presented.



CONCLUSIONS

In this paper we presented a comparative study about the performance of the Minimum Norm (MN), the Weighted Minimum Norm (WMN), the Minimum Laplacian (LORETA), LAURA and EPIFOCUS, in the localization of single sources without noise.

The two new solutions, LAURA and EPIFOCUS, produced the best results in terms of the number of sources with zero localization error, maximum localization error, and average localization error as a function of the source eccentricity. LAURA (32%) increased by 12 % the number of sources with zero localization error with respect to LORETA (20%). EPIFOCUS yielded a 95% of sources with zero localization error. The new methods reduce the maximum error from 5.48 (MN), 5.20 (WMN) and 3.16 (LORETA) down to 2.45 (LAURA) and finally to 1 (EPIFOCUS). The average error of LAURA is, except for one interval, better than MN, WMN and LORETA. The average error of EPIFOCUS is very close to zero for all eccentricity values.

The study of the performance of EPIFOCUS as a function of the number of electrodes shows for the first time that it is possible to obtain perfect localization (100%) with a relatively low number of electrodes (100 or more). Furthermore, the results of EPIFOCUS for noisy data, where the maximum error is not bigger than 2 grid units and the average error remains very close to zero, illustrate the robustness of this method. The robustness of this method to noise obeys to the fact that it is a quasi-solution, i.e., the data are not totally explained. The resulting effect is similar to the one produced by regularization procedures that try to increase the localization quality even if the predicted data differs from the measurements.

In summary, the behavior of EPIFOCUS with both synthetic noiseless and noisy data and experimental data indicate that we have at our disposal an accurate and computationally efficient tool for the localization of concentrated sources (not necessarily dipolar). As shown here, this is immediately applicable to the analysis of epileptic data with the advantage over single dipole models of being a method easy to implement in scattered solution spaces as the ones arising from segmentation of the individual subject MRI. The availability of high accurate localization methods as EPIFOCUS may become important in the future, for instance for identifying cases where amygdalo-hippocampectomy or other limited temporal lobe resections may replace the standard en bloc resections.

The comparative results described in this paper allow extracting some theoretical conclusions useful for the design and implementation of linear inverse solutions. That EPIFOCUS localizes all sources with zero dipole localization errors confirms that the dependence of the inverse matrix on the a priori information allows for the controlled adjustment of the columns of the resolution matrix, that is, the accurate retrieval of single sources, theoretically predicted in Grave and Gonzalez (1998). It

means that it is possible to design linear solutions with quasi-optimal performance in the determination of the position of single sources, i.e., the columns of the resolution matrix, can be adjusted at will to obtain quasi-optimal impulse responses (Grave and Gonzalez 1998) and thus, very low or even zero dipole localization errors.

The interpretable neurophysiological results obtained in a large variety of experimental event related data (Michel et al., 2001) support the choice of LAURA when the assumption of a single dominant source is not expected to hold. Still the constraints used in LAURA obey physically driven laws more likely to manifest with experimental data than with mathematically generated sources models such as the current dipole. However, the results of this paper indicate that this physically driven constraints are indeed a reasonable choice to deal with dipolar sources in the absence of any *a priori* information.

An additional theoretical conclusion derived from these results is that a lower dipole localization is neither a sufficient nor a necessary condition for the performance of a linear inverse solution. Moreover, EPIFOCUS and LAURA are particular cases of the WROP family (Grave et al, 1998) which demonstrate that the Weighted Resolution Optimization is an approach able to produce methods with bad single dipole localization properties such as the column Weighted Minimum Norm (WMN) but also optimal single source trackers as LAURA and EPIFOCUS.

While the analysis presented here considers only the electrical case, there is no theoretical reasons to expect different results for the magnetic case.

APPENDIX

For the researcher interested in testing concrete inverse solutions, we provide here all the mathematical details needed for their implementation.

LAURA (Local AUtoRegressive Average) solution

In Grave et al. (2000) we presented a new source model constrained by the physical properties of the generators of the electrical activity. This alternative source model (ELECTRA) allows the restatement of the bioelectric inverse problem in three mathematically equivalent ways. One of them transformed the original problem associated to the estimation of the current density vector (3D vector field) into the determination of the potential in depth (scalar field). Although the formulations described in ELECTRA are more restrictive, the solution is still non-unique, i.e., infinitely many solutions still exist. However, the physical properties of the unknown field (potential in depth) can also be considered to soundly pick up one of these solutions. The resulting solution strategy coined LAURA takes into account the physical features in the following way:

a) Since the potential in depth is scarcely determined by the external potential measurements, the resulting inverse problem is highly underdetermined. In other words, EEG measurements are not sufficient to fully determine the activity at all brain locations. Consequently, the electrical activity at each point can be expressed as a combination of the information supplied by the data and the local neighbors.

b) According to elementary potential theory, the Newtonian potential is a function of the inverse of the distance, electric potentials decays as a function of the square distance and the electric fields decays with the third power of the inverse distance

To include both aspects we express the activity at each point as a function of the neighbors by means of a local autoregressive estimator (Ripley, 1981) with coefficients that depend on the distance to the target point, that is,

$$f_i = \frac{N_i}{N} \sum_{k \in V_i} \frac{d_{ki}^{-e_i}}{\sum_{k \in V_i} d_{ki}^{-e_i}} f_k \quad (\text{A-1})$$

This equation express the unknown function value at the i -th point as a weighted sum of the unknown function values at the neighborhood as proposed in Grave and Gonzalez (1999). Since the sum of the weights is one, equation A-1 describes a consistent local average. The maximum number of neighbors is $N=26$ for a three-dimensional (3D) vicinity and N_i is the actual number of neighbors of point i . A neighborhood is defined by the hexaedron centered at the target point. Such selection allows for the consideration of solution spaces derived from anatomical images where the intergrid distances might differ in the three coordinate axes. For all solution points we use the same exponent $e_i=1$ or 2 or 3 to express the dependence with the distance

The factor N_i/N allows for the correct estimation of the constant function while incorporating into the formulation the fact that no primary sources exist outside the brain and consequently function values are zero outside brain borders.

Multiplying both sides by an arbitrary factor $w_i > 0$ and subtracting both sides of (A-1) and reorganizing we can obtain a new scalar field that defines implicitly a regularization operator (Grave and Gonzalez, 1999):

$$g_i = w_i \left\{ \frac{N}{N_i} \left[\sum_{k \in V_i} d_{ki}^{-e_i} \right] f_i - \sum_{k \in V_i} d_{ki}^{-e_i} f_k \right\} \quad (\text{A-2})$$

In other words, LAURA's approach minimizes the norm of the field g , which has components that are "spatially more independent" than those of f . One element of g

(nearly) zero implies that the corresponding element of f , is (almost) fully predicted from its neighbors (A-1) and not by the data.

Considering the discrete version of the problem:

$$d = L * J + n \quad (\text{A-3})$$

Where d stands for the data measured on n_s sensors, J is the discretization of the unknown function on n_p solution points and vector n represents the additive noise present in the data. The solution is obtained by solving the following variational problem for the unknown N_p -vector J .

$$\|d - LJ\| + \lambda * R(J) \quad (\text{A-4})$$

The regularization operator reads:

$$R(J) = \|WAJ\| \quad (\text{A-5})$$

According to (A-2), the diagonal element of the i -th row of A is:

$$A_{ii} = \frac{N}{N_i} \sum_{k \in V_i} d_{ki}^{-e_i} \quad (\text{A-6})$$

Where V_i stands for the vicinity of the i -th solution point and d_{ki} is the distance from the k -th neighbor to the target point i . The off-diagonal elements are zero except for $k \in V_i$ where the value is given by:

$$A_{ik} = -d_{ki}^{-e_i} \quad (\text{A-7})$$

When using the source model of ELECTRA (potential in depth), unless we have some additional information we set the diagonal matrix W to the identity and $e_i=2$.

For the estimation of the current density vector (vector field with 3 components), one can apply previous operator by components. In this case, the regularization operator reads:

$$R(J) = \|(WA \otimes I_3)J\| \quad (\text{A-9})$$

Where the symbol \otimes represents the kronecker product of matrices (Rao and Mitra, 1971), and the elements of the diagonal matrix W are selected as the mean of the

norm of the 3 columns of the lead field matrix associated with point i . This new weighting strategy increased significantly the localization capabilities of LAURA. While higher exponent values, e.g. $e_i=11$, can increase the number of sources perfectly localized up to 50%, in table I we consider only exponent values derived from potential theory, that is, $e_i=1,2$ and 3 .

With previous definitions the products $M=WA$ (scalar field) and $M=WA \otimes I_3$ (3D vector field) are invertible and the inverse matrix can be computed as:

$$G = (M^t M)^{-1} L^t [L(M^t M)^{-1} L^t + \lambda * I]^{-1} \quad (\text{A-10})$$

For an efficient numerical implementation of equation A-10 consider the following elements:

- According to the basic kronecker product properties (Rao and Mitra, 1971) only matrix $WA^t AW$ has to be inverted.
- Since all the matrices to be inverted are symmetric and positive definite then, compute only the upper triangles and use Cholesky algorithm for the inversion.
- Note that the product $(RR^t \otimes I_3) L^t$, where R is a Cholesky (triangular) factor of $(WA^t AW)^{-1}$, can be done without the explicit computation of the Kronecker product.

EPIFOCUS

Assuming that the data is generated by a single source and accepting (as is the case for all regularization algorithms) that the solution will not perfectly explain the data, we can obtain an inverse matrix highly sensitive to focal sources. The intuitive idea behind this method is to change the original problem to a new space (or variable) such that the projection over each location has an increased contrast power. For the mathematical implementation, note that the lead field has the following structure:

$$L = [L_1, L_2, \dots, L_{np}] \quad (\text{A-11})$$

where each block L_i is formed by ns rows and 3 columns associated with the potential generated by the three orthogonal unitary dipoles that can be placed at the i -th solution point. The two following steps produce the desired inverse matrix:

- Change of variable. Compute the transformed lead field matrix T by normalizing each column of L , i.e., $T=L * W$, where W is a diagonal matrix with elements equal to the inverse of the norm of the columns of L . Matrix T has the same structure of L , i.e.,

$$T = [T_1, T_2, \dots, T_{np}] \quad (\text{A-12})$$

b) Computing the local projectors. To obtain the inverse G , compute the Moore-Penrose pseudo inverse (Rao and Mitra, 1971) of each block and arrange them in the following way:

$$G = \begin{bmatrix} T_1^+ \\ T_2^+ \\ \vdots \\ T_{np}^+ \end{bmatrix} \quad (\text{A-13})$$

The product of this inverse matrix G with the recorded data yields an estimator of the weighted current source density. The plot of the modulus of this estimate for each solution point, can be interpreted (up to a scaling factor) as the probability of a focal source at that point. The column weighting used in the change of variable (step a), is essential for the localization features of EPIFOCUS and distinguishes it from other projectors used so far. While this weighting corresponds to the widely used column Weighted Minimum Norm (Lawson and Hanson, 1974), it has never been applied to the case of projectors as in equation (A-13).

References

- Ary, J.P., Klein, S.A. and Fender, D.H. Location of sources of evoked scalp potentials: corrections for skull and scalp thickness. *IEEE Trans. Biomed. Eng.* 1981, 28:447-452.
- Berg, P. and Scherg, M. A fast method for forward computation of multiple-shell spherical head models. *Electroencephalography and clinical Neurophysiology.* 1994,90: 58-64.
- Fuchs M, Wagner M, Köhler T, Wischmann H-A. Linear and nonlinear current density reconstructions. *J. Clin. Neurophysiol* 1999;16:267-95
- Golberg, M.A., (Ed.). *Solution Methods for Integral Equations*, Plenum Press, New York. 1978.
- Goronidnitsky, I.F., Rao, BD (1997) Spatial signal reconstruction from limited data using FOCUS: a reweighted minimum norm algorithm. *IEEE Trans. Sig. Proc.*, 45 (3)" 1-16.
- Grave de Peralta Menendez R, Hauk O, Gonzalez Andino, S, Vogt H and Michel. CM. Linear inverse solutions with optimal resolution kernels applied to the electromagnetic tomography. *Human Brain Mapping* 5, 1997, 454-467.

Grave de Peralta Menendez R, Gonzalez Andino S and Lütkenhöner B. Figures of merit to compare linear distributed inverse solutions. *Brain Topography*, 9, 117-124, 1996.

Grave de Peralta Menendez R, Gonzalez Andino SL. Distributed source models: Standard solutions and new developments. In: Analysis of neurophysiological brain functioning. Uhl, C. (Ed.). Springer Verlag, 1999, pp. 176-201.

Grave de Peralta Menendez R, Gonzalez Andino SL. A critical analysis of linear inverse solutions. *IEEE Trans Biomed Eng* 1998, 4: 440-48.

Grave de Peralta Menendez R, Gonzalez Andino SL, Morand S, Michel, CM, Landis TM. Imaging the electrical activity of the brain: ELECTRA. *Human Brain Mapping*, 2000, 1. 1:12.

Grave de Peralta Menendez, R. (1998) Linear Inverse solutions to the Neuroelectromagnetic Inverse Problem. PhD. Thesis NO. 3042. Faculty of Sciences. Geneva University. Geneva. Switzerland

Grave de Peralta Menendez R, Gonzalez, S.L. Discussing the capabilities of laplacian minimization. *Brain Topography* 2000, 13(2):97-104, Winter 2000

Grave de Peralta, R, Gonzalez, S.L, Lantz, G, Michel, C.M, Landis, T. Noninvasive localization of electromagnetic epileptic activity. I Method descriptions and simulations. *Brain Topography* 2001. In press.

Hämäläinen MS and Ilmoniemi RJ (1984): Interpreting measured magnetic fields of the brain: Estimates of current distributions. Technical Report TKK-F-A559, Helsinki University of Technology

Huiskamp G, van Oosterom A. The depolarization sequence of the human heart surface computed from measured body surface potentials. *IEEE Trans Biomed Eng*. 1988; 35:1047-58.

Lantz, G, Holub, M, Ryding, E, Rosen I. Simultaneous intracranial and extracranial recording of epileptiform activity in patients with drug resistant partial epilepsy: patterns of conduction and results from dipole reconstruction. *Electroenceph. Clin. Neurophysiol.* 1996, 99: 69-78.

Lantz, G, Michel, C.M, Pascual-Marqui, R.D, Spinelli, L, Seek, M, Landis, T, Rosen, I. *Electroenceph. Clin. Neurophysiol.* 1997, 102:414-422.

Lantz, G, Grave de Peralta, R, Gonzalez, S, Michel, C. M. Noninvasive localization of electromagnetic epileptic activity. II. Demonstration of sublobar accuracy in patients with simultaneous surface and depth recordings. *Brain Topography* 2001a, 14, 139-147.

Lantz G, Spinelli L, Grave de Peralta R, Seeck M, Michel CM. Tomographie électrique en épilepsie : localisation de sources distribuées et comparaison avec l'IRMf. *Epileptic Disorders* Vol 3, Special Issue No 1, 2001b.

Lawson C.L. and Hanson, R.J. (1974): *Solving least squares problems*. (Prentice Hall, Inc., Englewood Cliffs, New Jersey).

Menke W. *Geophysical data analysis: Discrete inverse theory*. Academic Press. San Diego. 1989

Messinger-Rapport, B.J. and Rudy, Y. Regularization of the inverse problem in electrocardiography: a model study. *Math Biosci.* 1988, 89:79-118.

Michel, C. M. Thut, G. Morand, S. Khateb, A. Pegna, A.L. Grave de Peralta, R. Gonzalez, S.L. Seeck, M. and Landis, T. Electric source imaging of human brain functions. *Brain Research Reviews*, 2001, In press.

Moore, E. H., 1920, *Bull.Amer.Math.Soc.*, 26, 394-395.

Philips, D. L. A technique for the numerical solution of certain integral equations of the first kind. *J. Assoc. Comput. Mach.* 1962, 9, 84-97.

Penrose, R., 1955a, A generalized inverse for matrices: *Proc.Cambridge Philos.Soc.*, 51, 406-413.

Penrose, R., 1955b, On best approximation solutions of linear matrix equations: *Proc.Cambridge Philos.Soc.*, 52, 17-19.

Pascual Marqui RD, Michel CM and Lehmann D. Low resolution electromagnetic tomography: a new method for localizing electrical activity in the brain. *Int. J. Psychophysiol.* 1995, 18: 49-65.

Rao, C.R. and Mitra, S.K. *Generalized inverse of matrices and its applications*. John Wiley & Sons, Inc., New York. 1971.

Ripley, B.D. *Spatial Statistics*, Wiley, New York, 1981.

Spinelli L, Lantz.G, Gonzalez, S.L., Michel CM. Anatomically constrained spherical head model for EEG source localization. *Brain Topography*, 13, 115-125, 2000.

Stok, C.J. *The inverse problem in EEG and MEG with application to visual evoked responses*. CIP Gegevens Koninklijke Bibliotheek, The Hague, 1986.

Tihonov, A.N. and Arsenin, V.Y. *Solutions of ill-posed problems*. Wiley, New York. 1997.

van Oosterom, A. History and evolution of methods for solving the inverse problem. *J. Clinical Neurophysiology*, 1992, 8:371-380.

Wagner, M. Fuchs, M. Wischmann, H.A., Drenckhahn, R., Köhler, T. Smooth reconstructions of cortical sources from EEG and MEG recordings. *Neuroimage* 1996, 3:168.

Wahba, G. Spline models for observational data. Society for Industrial and applied mathematics. Philadelphia. Pennsylvania. 1990.